

2.2 Ocean Drilling Perspectives on Meteorite Impacts

Christopher Lowery*¹, Joanna V. Morgan², Sean P.S. Gulick¹, Timothy J. Bralower³, Gail L. Christeson¹, Exp. 364 Scientists⁴

¹University of Texas Institute for Geophysics, Jackson School of Geosciences, Austin, USA

²Department of Earth Science and Engineering, Imperial College, London, UK

³Department of Geosciences, Pennsylvania State University, University Park, USA

⁴see list of science party members at the end

*corresponding author: cmlowery@utexas.edu; Research Associate, University of Texas Institute for Geophysics, JJ Pickle Research Campus 10100 Burnet Rd., Austin, TX, 78758
ORCID: <https://orcid.org/0000-0002-0101-4397>

Abstract

Extraterrestrial impacts are one of the most ubiquitous processes in the solar system, reshaping the surface of rocky bodies of all sizes. On early Earth, impact structures may have been a nursery for the evolution of life. More recently, a large meteorite impact caused the end Cretaceous mass extinction, killing 75% of species on the planet, including non-avian dinosaurs, and clearing the way for the dominance of mammals and eventual evolution of humans. Understanding the fundamental processes associated with impact events is critical to understanding the history of life on Earth and the potential for life across the solar system and beyond.

Scientific ocean drilling has generated irreplaceable data on impact processes. The Chicxulub impact is the single largest and most significant impact event that can be studied by sampling modern ocean basins, and marine sediment cores have been instrumental in quantifying the climatological and biological effects of the impact. Recent drilling in the Chicxulub Crater has already significantly advanced our understanding of fundamental impact processes, notably the formation of peak rings in large impact craters. These results raise a number of new questions waiting to be addressed with further drilling.

Extraterrestrial impacts have been controversially suggested as drivers for many important paleoclimatic events in the Cenozoic, up to and including the Younger Dryas stadial at the end of the last glacial maximum. However, marine sediment archives (e.g., Osmium

32 isotopes) provide a long term archive of major impact events in recent Earth history and show
33 that, other than the end Cretaceous, major paleoclimatic events are not driven by impacts.

34

35 **Keywords:** Ocean Drilling, Impact Events, Cretaceous-Paleogene, Chicxulub, Mass Extinction

36

37

38 **1 Introduction**

39 Large meteorite impacts have had a significant influence on Earth history, possibly
40 driving the early evolution of life (e.g., Kring, 2000; Nisbet and Sleep, 2001; Kring, D.A., 2003)
41 and the composition of the oceans and atmosphere (e.g., Kasting 1993). They also have the
42 potential to completely reshape the terrestrial biosphere (e.g., Alvarez et al., 1980). The
43 Cretaceous-Paleogene (K-Pg) mass extinction, caused by the impact of a meteorite on the
44 Yucatán carbonate platform of Mexico 66 Ma, is the most recent major mass extinction. It ended
45 the dominance of non-avian dinosaurs, marine reptiles, and ammonites, and set the stage for the
46 Cenozoic dominance of mammals that led directly to the evolution of humans (Schulte et al.,
47 2010; Meredith et al., 2011). This mass extinction was likely a direct response to climate change
48 over days to years, and thus provides an important partial analog for the recovery of biodiversity
49 following modern anthropogenic climate change.

50 The K-Pg impact hypothesis was controversial when first proposed, but careful
51 correlation of K-Pg boundary sections led to its gradual acceptance. The discovery of the
52 Chicxulub Crater in 1991 and its clear genetic relationship with K-Pg boundary ejecta provided
53 confirmation of this hypothesis (Hildebrand et al., 1991; Sigurdsson et al., 1991). Scientific
54 ocean drilling has been instrumental in discovering and documenting the global environmental
55 effects of the impact. Recent drilling by IODP Expedition 364 into the Chicxulub Crater itself
56 has yielded valuable insights into the mechanisms of large impact crater formation and the
57 recovery of life (Morgan et al., 2016; Lowery et al., 2018).

58 Although the K-Pg is the only mass extinction that is widely accepted to be caused by an
59 extraterrestrial collision, impacts have been suggested at one point or another as drivers for every

60 major extinction event (e.g., Rampino and Stothers, 1984) and many other major climate events
61 (e.g., Kennett et al., 2009; Schaller et al., 2016). The discovery of an iridium layer at the K-Pg
62 boundary as signature of extraterrestrial material spurred the search for other impact horizons
63 through the careful examination of many other geologically significant intervals, and so far no
64 other geologic event or transition has met the criteria to indicate causation by an impact (e.g., the
65 presence of Ir and other platinum group elements in chondritic proportions; tektites, shock-
66 metamorphic effects in rocks and minerals; perturbation of marine Os isotopes; and, ideally, an
67 impact crater).

68 The Deep Sea Drilling Project (DSDP), Ocean Drilling Program (ODP), Integrated
69 Ocean Drilling Program, and International Ocean Discovery Program (IODP) have provided a
70 unique and irreplaceable perspective on the history of the Earth for 50 years. IODP and its sister
71 organization the International Continental scientific Drilling Program (ICDP) provide insights
72 into impact cratering processes and effects of different magnitude events as well as target rocks
73 on the climate and biosphere, providing an exceptional record of processes that are ubiquitous
74 across the solar system (and, presumably, beyond). Here we examine the contributions of
75 scientific ocean drilling into our understanding of impact events, from detailed records of
76 extinction and chemical perturbation in the marine realm to the mechanisms by which rocks are
77 deformed to create peak rings in impact craters. The exciting results of recent drilling in the
78 Chicxulub crater raise new questions, and suggest promising new challenges and avenues of
79 investigation that can only be undertaken by a program like IODP.

80 **2 Marine Record of Impacts**

81 Scientific ocean drilling excels at providing raw material to generate high-resolution
82 composite records of geochemical changes in the ocean through time. One of these proxies is the
83 isotopic ratio of osmium, which records flood basalt volcanism (e.g., Turgeon and Creaser,
84 2008), weathering flux (Ravizza et al., 2001), ocean basin isolation (e.g., Poirier and Hillaire-
85 Marcel, 2009), and, importantly for our purposes, impact events (Peucker-Ehrenbrink and
86 Ravizza, 2000, 2012; Paquay et al., 2008). Extraterrestrial impacts result in a strong, rapid
87 excursion to unradiogenic (i.e., negative) $^{187}\text{Os}/^{188}\text{Os}$ ratios (Koeberl, 1998; Reimold et al., 2014)
88 (Figure 1A). The only two such excursions in the Cenozoic are Chicxulub (Figure 1B) and the
89 late Eocene (35 Ma; Poag et al., 1994) Chesapeake Bay impact on the North American Atlantic

90 coastal plain (Fig 1C) (Robinson et al., 2009; Peucker-Ehrenbrink and Ravizza, 2012). Other
91 major climate events which are associated with proposed impacts, like the Paleocene-Eocene
92 Thermal Maximum (PETM; e.g., Schaller et al., 2016) (Figure 1D), Miocene Climate Transition
93 (Figure 1E), and Younger Dryas (e.g., Kennett et al., 2009) (Figure 1F) are not associated with
94 any clear excursion toward unradiogenic values, despite relatively high sample resolution. It
95 should be noted that the Chesapeake Bay impact is approximately an order of magnitude smaller
96 than the Chicxulub impact (Poag et al., 1992) and is not associated with any significant climatic
97 or biological perturbation. Despite this, the event has a significant Os isotope excursion (Fig.
98 1C). Thus, an impact strong enough to effect global climate, as has been proposed at various
99 important climatic horizons beyond the K-Pg, would be expected to leave a clear signature in the
100 Os record. Setting aside the debates about whether any particular event coincides with a bolide
101 impact, the lack of an Os isotopic excursion for any of these events calls into question the scale
102 of any proposed contemporaneous impacts, and thus their causal relationship with the events
103 they happen to coincide with.

104 **3 The Chicxulub Impact and Its Physical Effects**

105 The hypothesis that an impact caused the most recent major mass extinction (Smit and
106 Hertogen, 1980) was founded on elevated iridium levels in the K-Pg boundary clays within
107 outcrops in Spain, Italy and Denmark (Alvarez et al., 1980). The impact hypothesis was initially
108 quite widely dismissed, and one of the early objections was that iridium had only been measured
109 at a few sites across a relatively small area and that it was not deposited instantaneously (Officer
110 and Drake, 1985). Researchers then began to investigate and document other K-Pg boundaries
111 around the globe, many of which were DSDP drill sites (Fig. 2). High iridium abundances were
112 soon found at other sites (e.g. Orth et al., 1981; Alvarez et al., 1982), and the identification of
113 shocked minerals within the K-Pg layer added irrefutable proof that it was formed by an extra-
114 terrestrial impact (Bohor et al., 1984). When a high-pressure shock wave passes through rocks,
115 common minerals such as quartz and feldspar are permanently deformed (referred to as shock
116 metamorphism), producing diagnostic features (e.g. Reimold et al., 2014) that are only found on
117 Earth in association with impacts and nuclear test sites. Since 1985, many ODP and IODP drill
118 sites have penetrated (and often specifically targeted) the K-Pg boundary (Fig. 2), further
119 contributing to our understanding of this event, and demonstrating that ejecta materials were
120 deposited globally (Figure 3).

121 The Chicxulub impact structure, Yucatán Peninsula, Mexico, was first identified as a
122 potential impact crater by Penfield and Carmargo (1981), and then as the site of the K-Pg impact
123 by Hildebrand et al. (1991). Hildebrand et al. (1991) noted that the size of the shocked quartz and
124 thickness of the K-Pg boundary deposit increased towards the Gulf of Mexico, and located the
125 Chicxulub crater due to its association with strong, circular, potential field anomalies. Core
126 samples from onshore boreholes drilled by Petróleos Mexicanos (“Pemex”) confirmed its impact
127 origin. Although Keller et al. (2004, 2007) argue against a link between Chicxulub and the K-Pg
128 boundary, accurate $^{40}\text{Ar}/^{39}\text{Ar}$ dating of impact glass within the K-Pg layer (Renne et al., 2013;
129 2018), as well as dating of shocked zircon (Krogh et al., 1993; Kamo et al., 2011) and
130 microcrystalline melt rock (Swisher et al., 1992) from Chicxulub and the K-Pg layer clearly
131 demonstrate that Chicxulub is the site of the K-Pg impact. Hildebrand et al. (1991) also noted that
132 DSDP Sites 94, 95, 536 and 540 contained deep water gravity flows and turbidity-current deposits
133 adjacent to the Campeche bank, and DSDP sites 603B, 151 and 153, as well as outcrops along the
134 Brazos River in Texas had potential tsunami wave deposits (Bourgeois et al., 1988), all of which
135 they suggested were caused by the Chicxulub impact.

136 Many studies have subsequently confirmed that, at sites proximal to Chicxulub, the impact
137 produced multiple surge, tsunami, gravity flow and shelf collapse deposits, some of which are
138 many meters thick (e.g. Bohor and Betterton, 1993; Bralower et al., 1998; Grajales-Nishimura et
139 al., 2000; Schulte et al., 2010; Vellekoop et al., 2014). Within the Gulf of Mexico basin, well logs,
140 DSDP cores, and seismic data show margin collapse deposits reach 100s of meters thick locally,
141 making the K-Pg deposit in the circum-Gulf of Mexico the largest known single event deposit
142 (Denne et al., 2013; Sanford et al., 2016). Complex stratigraphy (Figure 3) and a mixture of
143 nanofossil and foraminiferal assemblages of different ages and impact-derived materials
144 characterize proximal deep water DSDP and ODP sites in the Gulf of Mexico (DSDP Sites 95,
145 535, and 540), and Caribbean (ODP Sites 999 and 1001) driven by the sequential deposition of
146 material from seismically driven tsunami, slope collapse, gravity flows and airfall (Bralower et al.,
147 1998; Denne et al., 2013; Sanford et al., 2016). This distinct assemblage of materials was termed
148 the K-Pg “Boundary Cocktail” by Bralower et al. (1998).

149 At intermediate distances from Chicxulub (2000-6000 km) the K-Pg boundary layer is 1.5
150 – 3 cm thick, as seen in North America (Smit et al., 1992), the Demerara Rise (western Atlantic)
151 ODP Site 1207 (MacLeod et al., 2007; Schulte et al., 2009) and Gorgonilla Island, Columbia

152 (Bermúdez et al., 2016), and, at the first two locations, has a dual layer stratigraphy. The lower
153 layer contains goyazite and kaolonite spherules, which have splash-form morphologies such as
154 tear drops and dumbbells (Bohor et al., 1989; Smit and Romein, 1985; Bohor et al., 1993; Bohor
155 and Glass, 1995). The similarity between spherules in Haiti (~800 km from Chicxulub) and the
156 lower layer in North America has led to their joint interpretation as altered microtektites, which
157 were formed from ejected melt droplets (Smit and Romein, 1985; Bohor et al., 1993; Bohor and
158 Glass, 1995). Large-scale mass wasting has also been documented along the North Atlantic
159 margins of North America and Europe, including at Blake Plateau (ODP Site 1049), Bermuda Rise
160 (DSDP Sites 386 and 387), the New Jersey margin (DSDP Site 605), and the Iberian Abyssal Plain
161 (DSDP Site 398) (Klaus et al., 2000; Norris et al. 2000).

162 At distal sites (> 6000 km) the K-Pg boundary becomes a single layer with a fairly uniform
163 2-3 mm thickness, and has a similar chemical signature to the upper layer in North America (e.g.
164 Alvarez et al. 1982; Rocchia et al., 1992; Montanari and Koeberl, 2000; Claeys et al., 2002). The
165 most abundant component (60-85%) of the distal ejecta layer is spherules with a relict crystalline
166 texture (Smit et al., 1992) which are referred to as microkrystites (Glass and Burns, 1988), and are
167 thought to have been formed from liquid condensates within the expanding plume (Kyte and Smit,
168 1986). These microkrystites are now primarily composed of clay (smectite, illite, and limonite)
169 owing to their ubiquitous alteration. Some spherules contain skeletal, magnesioferrite spinel (Smit
170 and Kyte 1984; Kyte and Smit, 1986; Robin et al., 1991); spinel is the only pristine phase that
171 appears to have survived diagenetic alteration (Montanari et al., 1983; Kyte and Bostwick, 1995).
172 Shocked minerals are present in the K-Pg layer at all distances from Chicxulub, and are co-located
173 with the elevated iridium (Smit, 1999).

174 DSDP, ODP, and IODP sites (Fig. 2) have all been used for mapping the global properties
175 of the K-Pg layer. Sites close to the crater appear to have a slightly lower total iridium flux at 10 -
176 $45 \times 10^{-9} \text{ g cm}^{-2}$ (e.g. Rocchia et al., 1996; Claeys et al., 2002; MacLeod et al., 2007) compared
177 with a global average of $\sim 55 \times 10^{-9} \text{ g cm}^{-2}$ (Kyte, 2004), and maximum iridium concentrations are
178 quite variable (< 1 to > 80 ppb, Claeys et al., 2002). Although several attempts have been made to
179 locate the ultimate source of the iridium, the host is too fine-grained to be identified with
180 conventional techniques. The siderophile trace elements in the distal and upper K-Pg layer have a
181 chondritic distribution (Kyte et al., 1985), the isotopic ratio of the Platinum Group Element (PGE)

182 osmium is extra-terrestrial (Meisel et al., 1995), and the chromium isotopic composition indicates
183 the impactor was a carbonaceous chondrite (Shukolyukov and Lugmair, 1998).

184 The most common explanation for the origin of the microtektites at proximal and
185 intermediate sites is that they are formed from melted target rocks that have been ejected from
186 Chicxulub as melt droplets on a ballistic path within an ejecta curtain, and solidified en route to
187 their final destination (e.g. Pollastro and Bohor, 1993; Alvarez et al., 1995). Ejecta at distal sites
188 and within the upper layer at intermediate sites, including the shocked minerals and microkrystites,
189 are widely thought to have been launched on a ballistic trajectory from a rapidly expanding impact
190 plume (Argyle, 1989; Melosh et al., 1990). There are, however, several observations that are
191 difficult to reconcile with these explanations of how K-Pg ejecta traveled around the globe. For
192 example: 1) microkrystites within the global layer have roughly the same mean size (250 μm) and
193 concentration (20,000 per cm^2) (Smit, 1999), whereas shocked minerals show a clear decrease in
194 number and size of grains with increasing distance from Chicxulub (Hildebrand et al., 1991;
195 Crook et al., 2002); 2) if shocked quartz were ejected at a high enough velocity to travel to the
196 other side of the globe, the quartz would anneal on re-entry (Alvarez et al., 1995; Crook et al.,
197 2002); and 3) if the lower layer at intermediate sites were formed from melt droplets ejected from
198 Chicxulub on a ballistic path, the thickness of the lower layer would decrease with distance from
199 Chicxulub whereas, across North America, it is close to constant. Interactions of ejecta with the
200 Earth's atmosphere appear to be necessary to explain all of these observations (Goldin and Melosh,
201 2007; 2008; Artemieva and Morgan 2009; Morgan et al., 2013).

202 Differences in the K-Pg boundary layer around the globe have been used to infer different
203 angles and directions for the Chicxulub impactor. Schultz and D'Hondt (1996) argued that several
204 factors, including the dual layer and particularly large fragments of shocked quartz in North
205 America, indicated an impact direction towards the northwest. Subsequently, however,
206 comparable 2-cm thick K-Pg layers at sites to the south of Chicxulub at equivalent paleodistances
207 were identified (Schulte et al., 2009; Bermúdez et al., 2016), and it now appears that the global
208 ejecta layer is roughly symmetric, with the number and size of shocked quartz grains decreasing
209 with distance from Chicxulub (Crook et al., 2002; Morgan et al., 2006). One aspect of the layer
210 that is asymmetric is the spinel chemistry: spinel from the Pacific (e.g., DSDP Site 577) is
211 characterized by higher Mg and Al compared to European (e.g., Gubbio, Italy) and Atlantic spinel

212 (e.g., DSDP Site 524) (Kyte and Smit, 1986). Kyte and Bostwick (1995) concluded that the Pacific
213 spinel represented a higher temperature phase, and thus that the impact direction must have been
214 towards the west because the plume would be hottest in the downrange direction. Subsequently,
215 Ebel and Grossman (2005) used thermodynamic models to predict the sequential condensation
216 within the cooling impact plume and concluded the opposite: that the spinel from Europe and the
217 Atlantic represented the higher temperature phases and, thus, that the impact direction was towards
218 the east. Arguments that sought to use position of crater topography relative to the crater center
219 (Schultz and D'Hondt, 1996) have been questioned through comparisons with Lunar and Venutian
220 craters with known impact trajectories (Ekholm and Melosh, 1998; McDonald et al., 2008). More
221 recently, 3D numerical simulations of crater formation, which incorporate new data from IODP
222 Site M0077 in the Chicxulub crater, indicate that an impact towards the southwest at a $\sim 60^\circ$ angle
223 produces the best match between the modeled and observed 3D crater structure (Collins et al.,
224 2017).

225 **4 Ocean Drilling Perspective on Mass Extinction**

226 Paleontologists had long recognized a major mass extinction at the end of the Cretaceous
227 with the disappearance of non-avian dinosaurs, marine reptiles, and ammonites, although the first
228 indication of the rapidity of this event came from microfossils. The earliest advances on the
229 extinction of the calcareous and siliceous microfossils across the K-Pg boundary came from
230 outcrops on land (e.g., Luterbacher and Premoli-Silva, 1964; Perch Nielsen et al., 1982; Percival
231 and Fischer, 1977; Romein, 1977; Jiang and Gartner, 1986; Smit, 1982; Harwood, 1988; Hollis,
232 1997; Hollis et al., 2003). However, the full taxonomic scope of the extinction and how it related
233 to biogeography and ecology is largely known from ocean drilling (e.g., Thierstein and Okada,
234 1979; Thierstein, 1982; MacLeod et al., 1997; Pospichal and Wise, 1990; Bown et al., 2004). Deep-
235 sea sites also serve as the basis for our understanding of the subsequent recovery of life (Bown,
236 2005; Bernaola and Monechi, 2007; Jiang et al., 2010; Hull and Norris, 2011; Hull et al., 2011).
237 The K-Pg boundary has now been recovered in dozens of cores representing all of the major ocean
238 basins, including some from the earliest DSDP legs (Fig. 2) (Premoli Silva and Bolli, 1973; Perch-
239 Nielsen, 1977; Thierstein and Okada, 1979; see summary of key terrestrial sections in Schulte et
240 al., 2010). Deep-sea sections generally afford excellent microfossil preservation, continuous
241 recovery, and tight stratigraphic control including magnetostratigraphy and orbital chronology

242 (Röhl et al., 2001; Westerhold et al., 2008).

243 Studies of deep-sea sections have exposed the severity of the mass extinction among the
244 plankton with over 90% of foraminifera and nannoplankton species becoming extinct (Thierstein,
245 1982; D'Hondt and Keller, 1991; Coxall et al., 2006; Hull et al., 2011). These studies have also
246 shown that the extinction was highly selective, with siliceous groups experiencing relatively low
247 rates of extinction (Harwood, 1988; Hollis et al., 2003). Among the calcareous plankton groups,
248 survivors include high-latitude and near-shore species (Bown 2005; D'Hondt and Keller, 1991)
249 suggesting that these species were adapted to survive variable environments in the immediate
250 aftermath of the impact. Moreover, deep sea benthic foraminifera survived the impact with little
251 extinction, illustrating that deep ocean environments were not perturbed (Alegret et al., 2001;
252 2012). This is a strong piece of evidence in support of an extremely rapid extinction event, as
253 expected for an impact, as it must have occurred faster than the mixing time of the ocean (~1000
254 years). Benthic foraminifera would suffer an extinction 10 myr later during the Paleocene Eocene
255 Thermal Maximum (Thomas and Monechi, 2007), a geologically rapid event that was still slow
256 enough to impact the deep sea.

257 Carbon isotopes across the oceans appear to suggest that the flux of organic carbon to the
258 deep ocean ceased or was very low for ~3 myr, a phenomenon which was originally interpreted as
259 indicating the complete or nearly complete cessation of surface ocean productivity (Hsü and
260 McKenzie, 1985; Zachos et al., 1989; the latter from DSDP Site 577 on Shatsky Rise, a fertile
261 location for K-Pg studies). This hypothesis became known as the Strangelove Ocean (after the
262 1964 Stanley Kubrick movie) (Hsü and McKenzie, 1985). D'Hondt et al. (1998) suggested that
263 surface ocean productivity continued, but the extinction of larger organisms meant that there was
264 no easy mechanism to export this organic matter to the deep sea – a modification of the Strangelove
265 Ocean hypothesis that has since been known as the Living Ocean hypothesis. However, several
266 facts about the earliest Danian ocean are incompatible with both of these hypotheses. The lack of
267 a corresponding benthic foraminiferal extinction suggests that the downward flux of organic
268 carbon may have decreased somewhat but remained sufficiently elevated to sustain the benthic
269 community (Hull and Norris, 2011; Alegret et al., 2001). More recent work on biogenic barium
270 fluxes in deep sea sites across the world has shown that, in fact, export productivity was highly
271 variable in the early Danian, with some sites recording an *increase* in export production during the

272 period of supposed famine in the deep sea (Hull and Norris, 2011).

273 Calcareous plankton communities were geographically heterogeneous in the immediate
274 aftermath of the mass extinction (Jiang et al., 2010). Among the nanoplankton, northern
275 hemisphere assemblages are characterized by a series of high-dominance, low-diversity “boom-
276 bust” species (Bown, 2005); southern hemisphere assemblages contain a somewhat more diverse
277 group of surviving species (Schueth et al., 2015). In general, diversity of northern hemisphere
278 assemblages took longer to recover (Jiang et al., 2010) and heterogeneity was maintained for more
279 than 300 kyr. This heterogeneity is likely a result of a combination of factors including incumbency
280 of the surviving population in the southern hemisphere sites as well as environmental and
281 ecological differences following the impact (Schueth et al., 2015).

282 However, the shift in the surface-to-deep carbon isotope gradient does have significant
283 implications for biogeochemical cycling, and is still ultimately linked to a major disruption and
284 recovery of food webs across the oceans. In the pelagic realm, diminished productivity by
285 nanoplankton and increased bacterial activity (Sepulveda et al., 2009) combined with flourishing
286 production of calcisphere resting stages drastically changed the surface-to-deep carbon isotope
287 gradient (Kump, 1991) and led to an increase in carbonate saturation (Henehan et al., 2016).
288 Pelagic calcifiers like planktic foraminifera and calcareous nanoplankton are a key component of
289 the carbon cycle, exporting carbon in the form of CaCO_3 from the surface ocean to the seafloor,
290 where it is buried. The extinction of so many marine calcifiers, and the smaller size of the
291 survivors, led to the weakening of the marine “alkalinity pump” (Henehan et al., 2016), and the
292 resulting oversaturation can be observed in a white layer that overlies the K-Pg boundary in
293 numerous sites including the eastern Gulf of Mexico (DSDP Site 536; Buffler et al., 1984), the
294 Caribbean (ODP Sites 999 and 1001; Sigurdsson et al., 1997), Shatsky Rise in the western Pacific
295 (Fig. 3) (IODP Sites 1209-1212; Bralower et al., 2002), and in the Chicxulub Crater itself (IODP
296 Site M0077; Morgan et al., 2017).

297 Records from cores across the oceans indicate that the post-extinction recovery of export
298 productivity (e.g., Hull and Norris, 2011) and calcareous plankton diversity (e.g., Jiang et al., 2010)
299 was geographically heterogeneous, with some localities recovering rapidly and others taking
300 hundreds of thousands (for productivity) to millions (for diversity) of years to recover. Recovery
301 appears to be slower in the North Atlantic and Gulf of Mexico (e.g., Alegret and Thomas, 2005;

302 Jiang et al., 2010; Hull and Norris, 2011), suggesting that distance from the crater correlates to
303 slower recovery. Some authors (e.g., Jiang et al., 2010) attributed this to direct environmental
304 effects of the impact, such as perhaps the uneven distribution of toxic metals in the oceans. If this
305 is true, then the recovery from the K-Pg mass extinction is driven by impact-specific processes
306 and thus can only be used to understand impact-driven extinctions (i.e., just the K-Pg). If recovery
307 is slower closer to the crater, then it should be slowest in the crater itself. However, recent drilling
308 within the Chicxulub crater has shown a rapid recovery of life there, with planktic and benthic
309 organisms appearing within just a few years of the impact and a healthy, high productivity
310 ecosystem established within 30 kyr of the impact, much faster than other Gulf of Mexico and N.
311 Atlantic sites (Lowery et al., 2018). This rules out an environmental driver for heterogeneous
312 recovery and instead suggests that natural ecological factors like incumbency and competitive
313 exclusion (e.g., Hull et al., 2011; Schueth et al., 2015) governed the recovery of the marine
314 ecosystem. The recovery of diversity took millions of years to even begin to approach Cretaceous
315 levels (Coxall et al., 2006; Bown et al., 2004; Fraass et al., 2015). This delay in the recovery of
316 diversity appears to be a feature of all extinction events (Kirchner and Weil, 2000; Alroy, 2008)
317 and bodes ill for the recovery of the modern biosphere after negative anthropogenic impacts
318 associated with climate change, over fishing, hypoxia, etc. subside.

319 **5 Unique Insight into the Chicxulub Crater**

320 Joint IODP-ICDP Expedition 364 drilled into the peak ring of the Chicxulub impact crater
321 in 2016 at Site M0077 (Morgan et al., 2017). Peak rings are rings of elevated topography that
322 protrude through the crater floor in the inner part of large impact structures. Prior to drilling, there
323 was no consensus on the nature of the rocks that form peak rings or their formational mechanism
324 (Baker et al., 2016). To form large craters like Chicxulub, rocks must temporarily behave in a
325 fluid-like manner during crater formation (Melosh, 1977). Two hypotheses, developed from the
326 observation of craters on other planets, proposed explanations of the process by which peak rings
327 form. The first, the dynamic collapse model (first put forward by Murray, 1980) would predict that
328 the Chicxulub peak ring would be formed from deep crustal rock, presumably crystalline
329 basement. The second, the nested melt-cavity hypothesis (conceived by Cintala and Grieve, 1998),
330 would predict that the Chicxulub peak ring would be underlain by shallow crustal rock, presumably
331 Cretaceous carbonates. Thus, Expedition 364 was able to answer a major question about impact

332 cratering processes simply by seeing what kind of rock comprises the peak ring. Geophysical data
333 acquired prior to drilling indicate that there are sedimentary rocks several kilometers beneath the
334 peak ring at Chicxulub, and that the peak-ring rocks have a relatively low velocity and density,
335 suggesting that they are highly fractured (Morgan et al., 1997; Morgan and Warner, 1999; Gulick
336 et al., 2008, 2013; Morgan et al., 2011). Site M0077 sampled the peak ring at Chicxulub to study
337 the rocks that compose them, determine their physical state, better constrain the kinematics and
338 dynamics of large crater formation, and further understand the mechanism by which rocks are
339 weakened to allow bowl-shaped transient cavities to collapse and form relatively wide, flat craters
340 (Gulick et al., 2017).

341 Immediately after impact the peak ring was located adjacent to a thick sheet of impact melt
342 and Chicxulub was inundated with sea-water (Gulick et al., 2008, *in prep*). Thus, intense
343 hydrothermal activity within the peak ring is expected, which may have been associated with
344 mineralization and/or provided a niche for life forms, in a similar way to oceanic hydrothermal
345 vent systems (Abramov and Kring, 2007). Therefore, cores collected during Expedition 364 can
346 be used to address key questions about the potential habitability of large impact craters, an
347 important analog for early life on Earth. High microbe cell counts and DNA have been found in
348 the peak-ring rocks, demonstrating that the crater currently provides a habitat for a deep biosphere
349 (Cockell et al., *submitted*).

350 Site M0077 (Fig. 4) was drilled on the outer edge of the peak ring in a small topographic
351 valley where the uppermost peak-ring rocks are formed from a relatively thick (100-150 m)
352 sequence of material with an unusually low seismic velocity (Morgan et al., 2011; Gulick et al.,
353 2017). This site was selected in order to maximize the chance of recovering the earliest Paleocene,
354 obtain a thick section of the low-velocity material that was thought to be impact breccia, and
355 sample several hundred meters of rocks that form the upper peak ring. Coring started at ~500
356 meters below sea floor (mbsf) and ~110 m of Paleogene sedimentary rocks were recovered before
357 encountering the top of the peak ring, where an unusual 80-cm thick transitional unit lies above a
358 ~130-m thick sequence of suevite (impact melt bearing breccia) and impact melt rocks. Granitoid
359 basement rocks with pre- and post-impact dykes and suevitic intercalations were encountered from
360 ~748 mbsf to the bottom of the hole at 1335 mbsf (Morgan et al., 2016; 2017).

361 The discovery that the peak ring was formed from fractured, shocked, uplifted basement
362 rocks supports the dynamic collapse model of peak-ring formation (Morgan et al., 2016; Kring et
363 al., 2017). Structural data from the wireline logging, CT scans, and visual core descriptions provide
364 an exceptional record of brittle and viscous deformation mechanisms within the peak-ring rocks.
365 These data reveal how deformation evolved during cratering, with dramatic weakening followed
366 by a gradual increase in rock strength (Riller et al., *in review*). The peak-ring rocks have
367 extraordinary physical properties: the granitic basement has P-wave velocities and densities that
368 are, respectively, ~25% and ~10% lower than expected, and a porosity of 8-10%. These values are
369 consistent with numerical simulations that predict the peak-ring basement rocks represent some of
370 the most shocked and damaged rocks in an impact basin (Christeson et al., 2018). Site M0077
371 cores and measurements have been used to refine numerical models of the impact and new
372 estimates on the release of climatic gases by the Chicxulub impact. Previous models estimated 100
373 Gt of sulfur (which formed sulfate aerosols in the atmosphere, blocking incoming solar radiation)
374 were released by the impact, which resulted in a 26°C drop in global temperatures (Brugger et al.,
375 2017); new models indicate that between 195 and 455 Gt of sulfur were released, suggesting even
376 more radical cooling during the impact winter (Artemieva et al., 2017).

377 **6 New Challenges**

378 The scientific community's understanding of the Chicxulub impact event and the K-Pg
379 mass extinction has grown immensely since Alvarez et al. (1980) first proposed the impact
380 hypothesis, and many of the advances were the direct result of new ocean drilling data. However,
381 there is still a great deal that we do not know. New K-Pg boundary sites from undersampled regions
382 (the Pacific, the Indian Ocean, and the high latitudes) are essential to reconstruct environmental
383 gradients in the early Paleocene, understand geographic patterns of recovery and what drives them.
384 Site U1514, on the Naturaliste Plateau on the SW Australian margin (Fig. 2), was drilled in 2017
385 on Expedition 369 (Huber et al., 2018) and is a perfect example of the kind of new site we need to
386 drill; at a high latitude and far from existing K-Pg boundary records, it is sure to provide a new
387 perspective on a number of existing questions.

388 New data from the Chicxulub Crater have resulted in refined impact models that suggest
389 that the asteroid impacted towards the southwest (Collins et al., 2017) which contrasts with
390 previously inferred directions that placed the northern hemisphere in the downrange direction.

391 Although the most proximal Pacific crust at the time of impact has since been subducted, very
392 little drilling has been conducted on older crust in the central and eastern Pacific (red circle on Fig.
393 2). New drilling on seamounts and rises on the furthest east Cretaceous crust in the eastern
394 equatorial Pacific would shed new light on the environmental and biological consequences of
395 being downrange of the Chicxulub Impact.

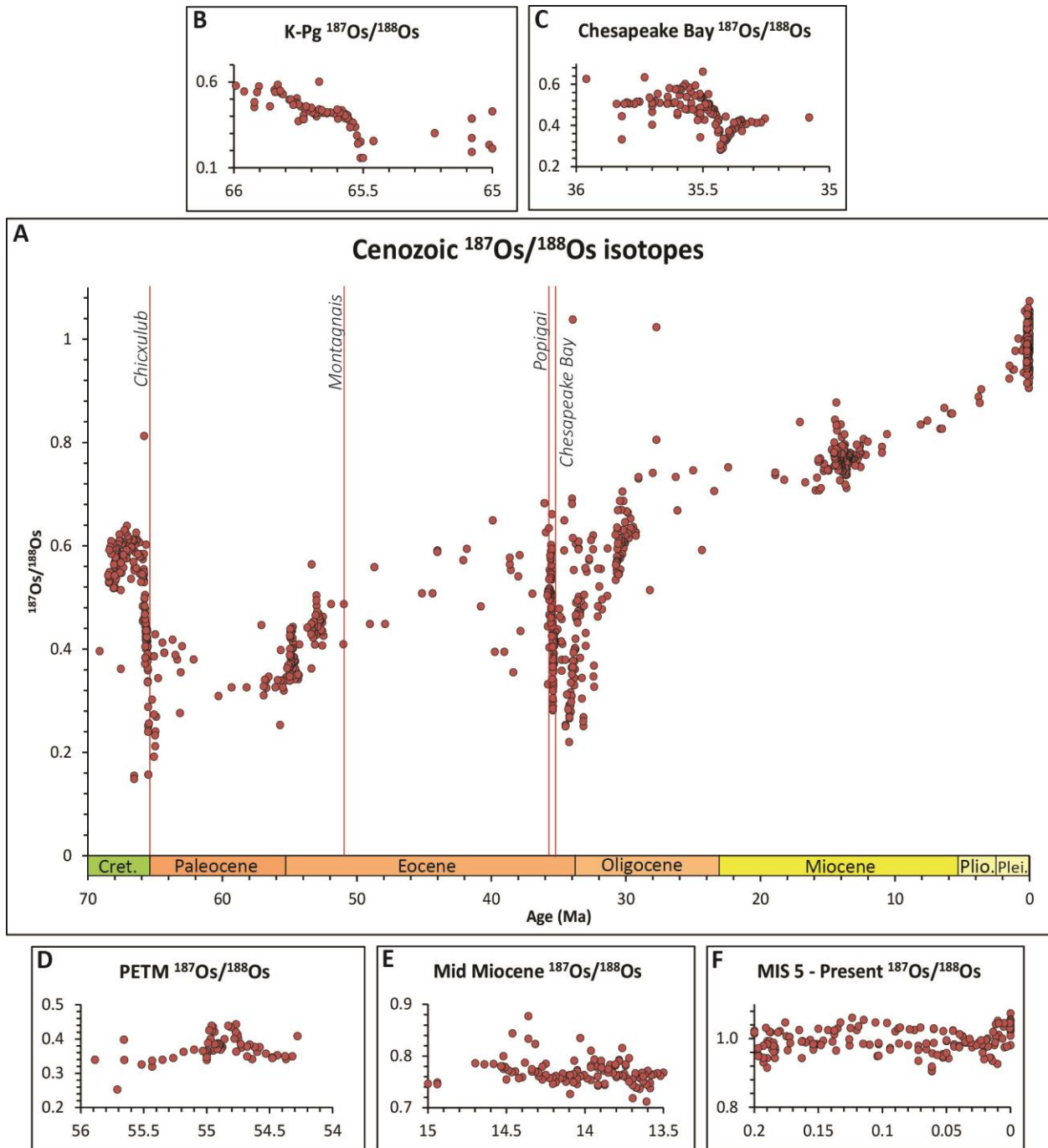
396 Finally, the Chicxulub structure remains an important drilling target to address questions
397 that can only be answered at the K-Pg impact site. Two particular locations will likely bring the
398 greatest return: the annular trough and the central basin. IODP Site M0077, which was drilled at
399 the location where the peak ring was shallowest, recovered a relatively thin Paleocene section with
400 an unconformity present prior to the Paleocene-Eocene boundary. Seismic mapping within the
401 crater demonstrates that the Paleocene section greatly expands into the annular trough (Fig. 4)
402 providing a potentially exciting opportunity to study the return of life to the impact crater at an
403 even higher resolution than presented in Lowery et al. (2018). Additionally, Expedition 364 has
404 raised new questions as to the quantity of sulfur-rich evaporites that remained in the impact crater
405 as opposed to being vaporized and released to the global environment through the vapor plume
406 (Gulick et al., *in prep*). The sedimentary target rock is 30-50% evaporites yet virtually none were
407 recovered at Site M0077; thus, it is key to have continuous coring within an expanded Paleocene
408 section and the underlying impactites to better constrain climatologic inputs at the onset of the
409 Cenozoic.

410 Equally intriguing is the interaction of impact melt rock, suevite, and post-impact
411 hydrothermal systems for studying how subsurface life can inhabit and evolve within an impact
412 basin. Such settings were common on early Earth and provide an analog for the chemical evolution
413 of pre-biotic environments as well as biologic evolution in extreme environments. Full waveform
414 images (Fig. 4) give tantalizing suggestions of vertical flux in the form of morphologic
415 complexities between the high-velocity melt sheet and overlying low velocity suevite layer, which
416 are tempting to interpret as hydrothermal vents, of the kind often seen at mid-ocean ridges. Drilling
417 into the Chicxulub melt sheet is ideal to study the hydrogeology and geomicrobiology of terrestrial
418 impact melt sheets buried by breccias as a habit for subsurface life, providing an opportunity for
419 scientific ocean drilling to sample the best analog for the habitat in which life may have formed
420 on early Earth and on rocky bodies across the solar system and beyond.

421 The success of the cooperation between IODP and ICDP during Expedition 364 should
422 serve as a model for future drilling in the Chicxulub crater as well as future Mission Specific
423 Platform (MSP) expeditions. The onshore Yaxcopil-1 borehole unexpectedly encountered a
424 Cretaceous megablock because it were essentially drilling blind, with only the regional magnetic
425 and gravity anomaly maps to guide it. High-quality marine seismic data from offshore portion of
426 the Chicxulub crater (Morgan et al., 1997; Gulick et al., 2008; Christeson et al., 2018) allowed for
427 a detailed characterization of the subsurface before drilling even began (Whalen et al., 2013). In
428 turn, this allowed Hole M0077A to precisely target not just the peak ring but a small depression
429 on top of the peak ring expected to contain earliest Paleocene sediments which provided the basis
430 for unprecedented study of this unique interval at ground zero (Lowery et al., 2018; Gulick et al.,
431 *in prep* and several other upcoming papers). As we plan for the next 50 years of scientific ocean
432 drilling, we should look for additional opportunities to leverage the clarity and resolution of marine
433 seismic data with the precision drilling possible from a stable platform provided by ICDP (Exp.
434 364 achieved essentially 100% recovery; Morgan et al., 2017).

435

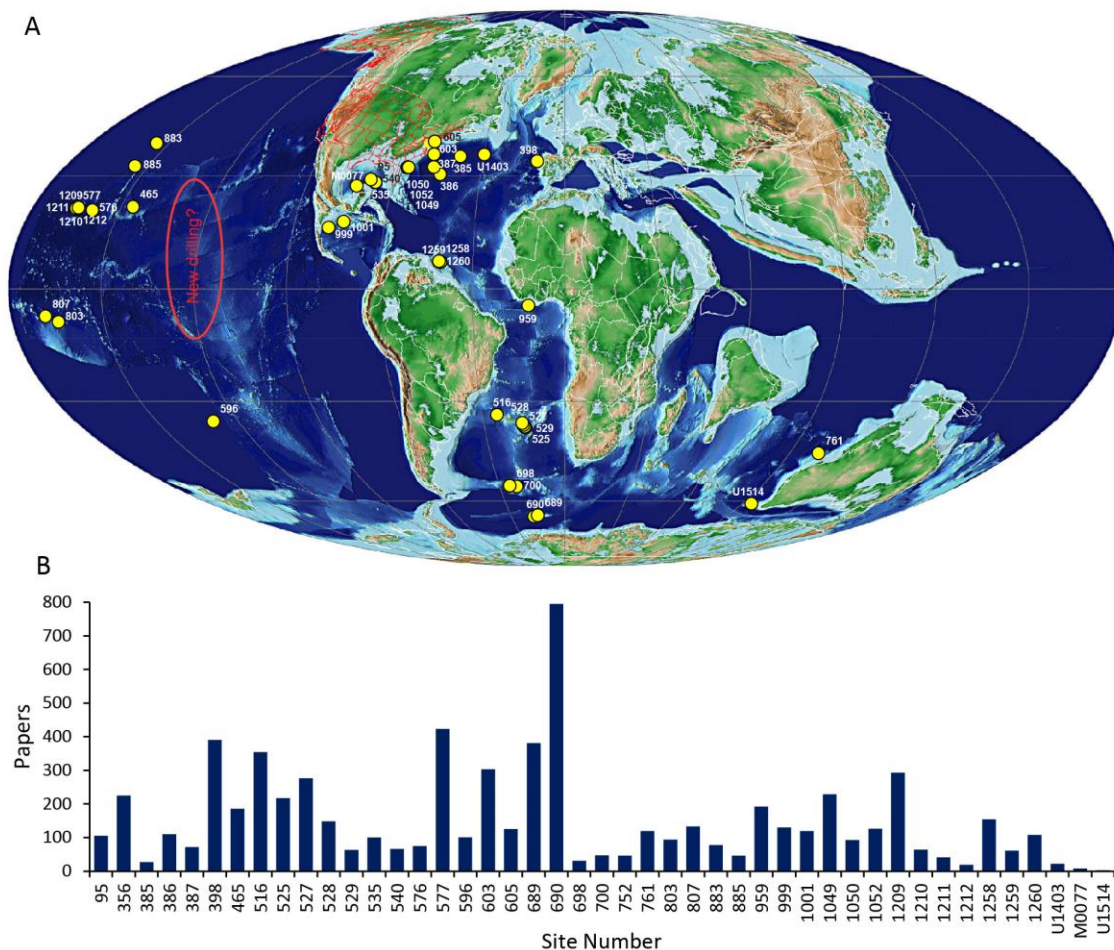
436



437

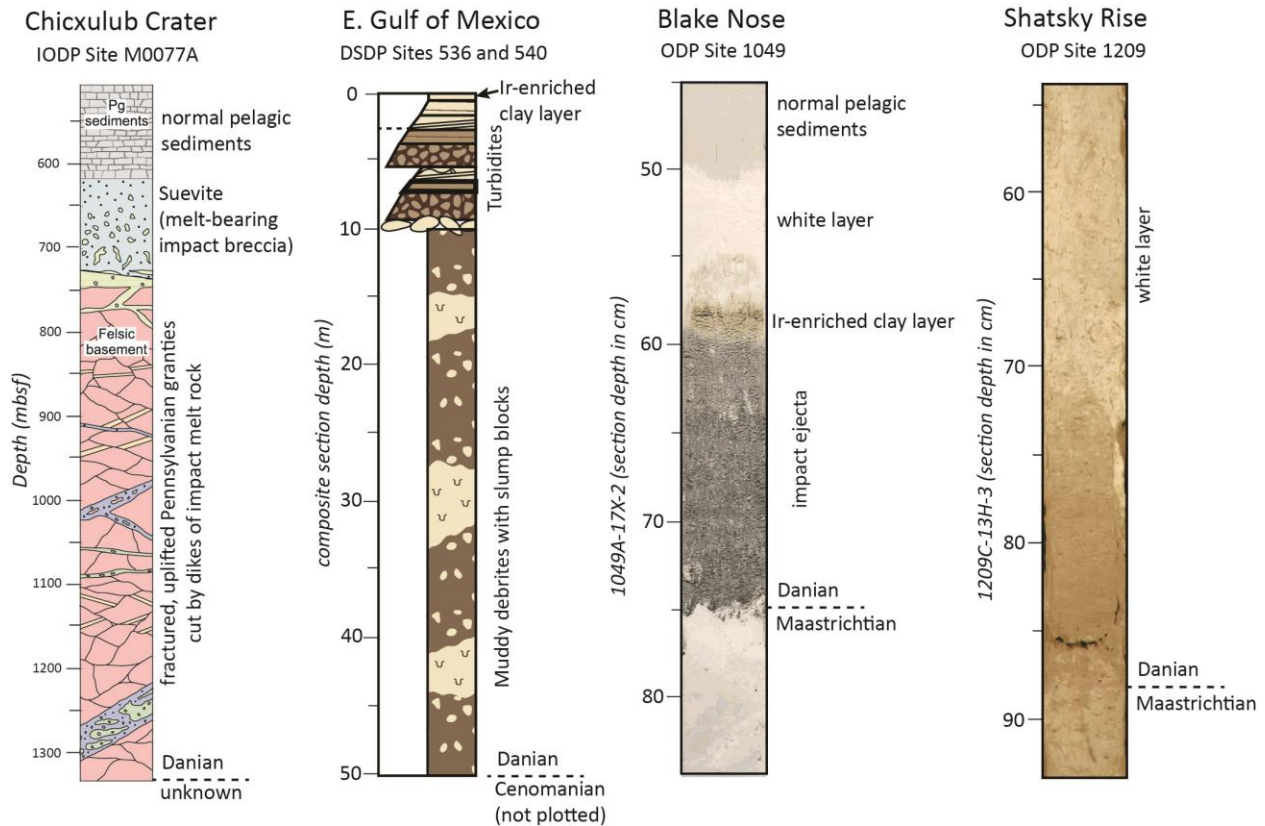
438 **Fig. 1** Marine osmium isotopes through the Cenozoic (a), after Peucker-Ehrenbrink and Ravizza
 439 (2012). These data, the majority of which come from DSDP/ODP/IODP cores, record the long-
 440 term trend toward more radiogenic (i.e., continental-weathering derived) $^{187}\text{Os}/^{188}\text{Os}$ ratios in the
 441 ocean throughout the Cenozoic. Superimposed on this long-term trend are several major, rapid
 442 shifts toward unradiogenic ratios driven by impact of extraterrestrial objects. This effect is evident
 443 in intervals associated with impact events, including the Chicxulub impact (b) and Chesapeake

444 Bay impact (c). Other intervals for which impacts have been proposed as important drivers of
 445 observed paleoclimatic change lack the diagnostic negative excursion, including the Paleocene
 446 Eocene Thermal Maximum (d), Miocene Climate Transition (e), and Younger Dryas (f). Red lines
 447 are well-dated large (>35 km crater diameter) impacts, after Grieve (2001).



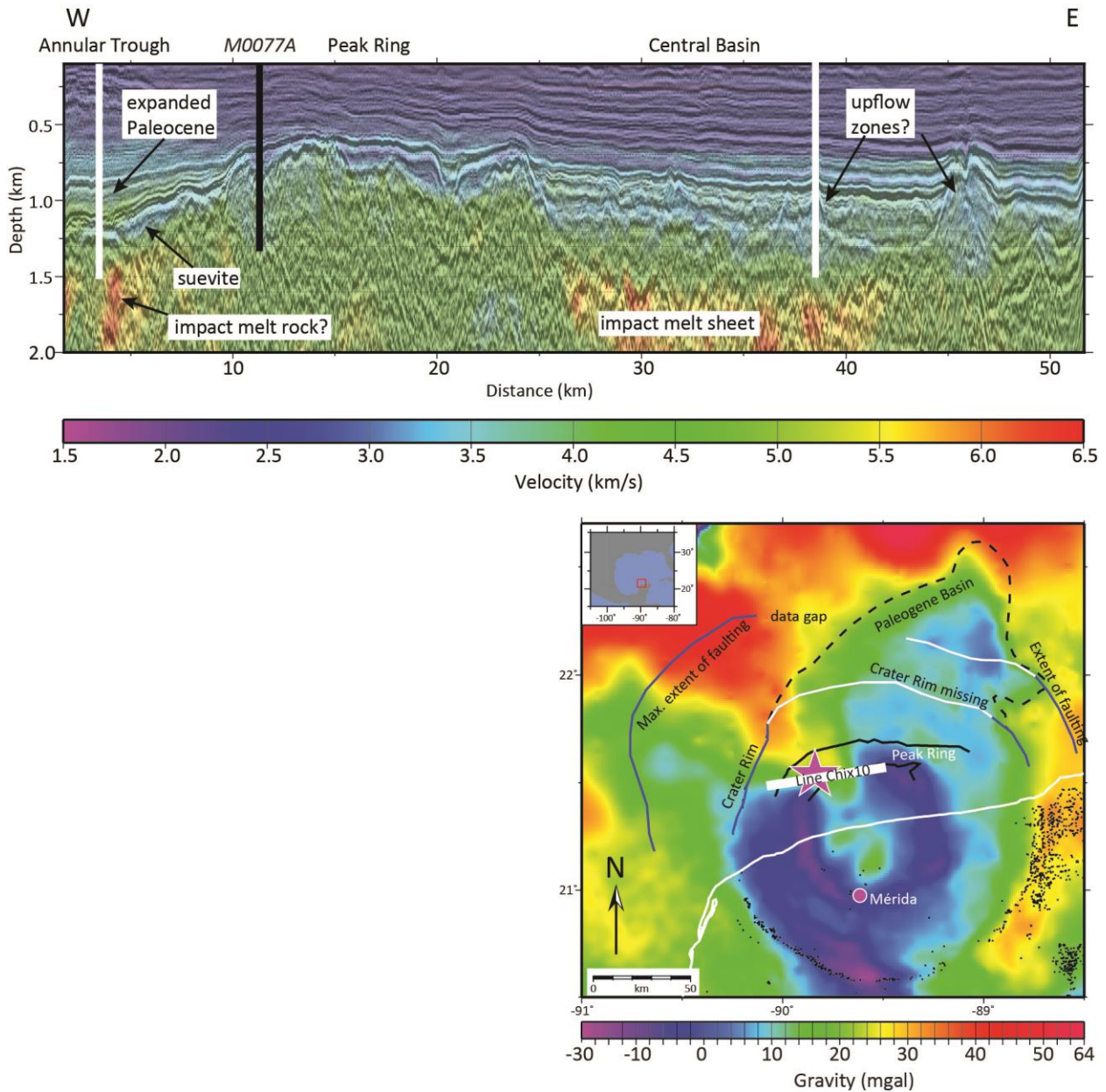
448 **Fig. 2 a)** Map of DSDP/ODP/IODP Sites which recovered the K-Pg boundary. Basemap is adapted
 449 from the PALEOMAP Project (Scotese, 2008) **b)** Number of K-Pg papers by site, according to
 450 Google Scholar as of July 5, 2018. As anyone who's looked up a paper on Google Scholar will
 451 recognize, there are some caveats with these data (e.g., inclusion of papers which match the search
 452 terms but are not strictly about the K-Pg, papers that are missing because they are not cataloged
 453 by Google Scholar, etc.). However, this is a good approximation of the reams of articles that have
 454 been written about the K-Pg from DSDP, ODP, and IODP cores, and the clear impact (sorry) of
 455

456 scientific ocean drilling on the K-Pg literature. n = 6797, but includes duplicates from papers which
 457 cover multiple sites. Search term: “Cretaceous AND Tertiary OR Paleogene OR Paleocene AND
 458 ‘Site ###’”.



459

460 **Fig. 3** Representative K-Pg boundary sections from scientific ocean drilling cores. Chicxulub
 461 crater is redrawn from Morgan et al. (2016), eastern Gulf of Mexico is redrawn from Sanford et
 462 al. (2016), Blake Nose and Shatsky Rise core photographs are from the Janus database.



463

464 **Fig. 4 (a)** Full wavefield inverted (FWI) velocity model (colors) and migrated seismic reflection
 465 image for profile CHIX 10 crossing site M0077 (black line). The seismic image has been converted
 466 to depth using the inverted velocity model. Potential sites for future drilling are shown with white
 467 lines. Drilling in the annular trough site would encounter an expanded Paleocene section, underlain
 468 by suevite (low velocities) and possible impact melt rock (high velocities). Coring in the central
 469 basin site would target an interpreted hydrothermal upflow zone (disrupted low-velocities) above
 470 the impact melt sheet (high velocities) as well as an expanded Paleocene section. **(b)** Location map

471 showing the gravity-indicated structure of the crater and the position of the seismic line used in A.
472 Modified from Gulick et al. (2008).

473

474 **Acknowledgements.** We would like to thank the editors for inviting us to contribute to this special
475 issue. We are also grateful to Bernhard Peucker-Ehrenbrink for sharing his Os isotope dataset and
476 Ian Norton and Jeremy Owens for help with the paleogeographic map projection.

477

478 **Expedition 364 Scientists**

479 Tim Bralower, Elise Chenot, Gail Christeson, Philippe Claeys, Charles Cockell, Marco J. L.
480 Coolen, Ludovic Ferrière, Catalina Gebhardt, Kazuhisa Goto, Sophie Green, Sean Gulick,
481 Heather Jones, David A. Kring, Johanna Lofi, Christopher Lowery, Claire Mellett, Joanna
482 Morgan, Rubén Ocampo-Torres, Ligia Perez-Cruz, Annemarie Pickersgill, Michael Poelchau,
483 Auriol Rae, Cornelia Rasmussen, Mario Rebolledo-Vieyra, Ulrich Riller, Honami Sato, Jan
484 Smit, Sonia Tikoo, Naotaka Tomioka, Jaime Urrutia-Fucugauchi, Michael Whalen, Axel
485 Wittmann, Long Xiao, and Kosei Yamaguchi.

486

487

488 **References**

489 Abramov, O., and Kring, D.A., 2007. Numerical modeling of impact-induced hydrothermal
490 activity at the Chicxulub crater. *Meteoritics & Planetary Science*, 42(1):93–
491 112. <http://dx.doi.org/10.1111/j.1945-5100.2007.tb00220.x>

492 Alegret, L., E. Molina, and E. Thomas (2001), Benthic foraminifera at the Cretaceous-Tertiary
493 boundary around the Gulf of Mexico, *Geology*, 29(10), 891-894.

494 Alegret, L., and Thomas, E. (2005). Cretaceous/Paleogene boundary bathyal paleo-environments
495 in the central North Pacific (DSDP Site 465), the Northwestern Atlantic (ODP Site 1049),
496 the Gulf of Mexico and the Tethys: The benthic foraminiferal record. *Palaeogeography,*
497 *Palaeoclimatology, Palaeoecology*, 224(1), 53-82.

498 Alegret, L., E. Thomas, and K.C. Lohmann (2012), End-Cretaceous marine mass extinction not
499 caused by productivity collapse, *Proceedings of the National Academy of Sciences*, 109(3),
500 728-732.

501 Alroy, J. (2008). Dynamics of origination and extinction in the marine fossil record, *PNAS* 105
502 11536-11542.

503 Alvarez, L.W., Alvarez, W., Asaro, F., Michel, H.V., 1980. Extraterrestrial cause of the
504 Cretaceous–Tertiary extinction. *Science* 208, 1095–1108.

- 505 Alvarez, W., L.W. Alvarez, F. Asaro and H.V. Michel. 1982. Current status of the impact theory
506 for the terminal Cretaceous extinction. In L. T. Silver and P. H. Schultz, eds., Geological
507 implications of impacts of large asteroids and comets on the Earth, Special Paper 190, pp.
508 305-315. Boulder, Colorado, Geological Society of America.
- 509 Alvarez, W., Claeys, P., Kieffer, S., 1995. Emplacement of Cretaceous–Tertiary boundary shocked
510 quartz from Chicxulub crater. *Science* 269, 930–935.
- 511 Argyle, E. 1989. The global fallout signature of the K-T bolide impact. *Icarus*, 77, 1, 220-222.
- 512 Artemieva, N., and J. Morgan (2009), Modeling the formation of the K-Pg boundary layer, *Icarus*,
513 201, 768-780.
- 514 Artemieva N. et al., 2017, Quantifying the Release of Climate-Active Gases by Large Meteorite
515 Impacts With a Case Study of Chicxulub, *Geophysical Research Letters*, ISSN: 0094-8276
- 516 Baker, D.M.H., J. W. Head, G. S. Collins, R. W. K. Potter, The formation of peak-ring basins:
517 Working hypotheses and path forward in using observations to constrain models of impact-
518 basin formation, *Icarus*, 273, 146 (2016).
- 519 Bermúdez, H.D., García, J., Stinnesbeck, W., Keller, G., Rodríguez, J.V., Hanel, M., Hopp, J.,
520 Schwarz, W.H., Tieloff, M., Bolivar, L., and Vega, F.J., 2016, The Cretaceous-Palaeogene
521 boundary at Gorgonilla Island, Colombia, South America: *Terra Nova*, v. 28, p. 83–90,
522 <https://doi.org/10.1111/ter.12196>
- 523 Bernaola, G., and S. Monechi (2007), Calcareous nannofossil extinction and survivorship across
524 the Cretaceous– Paleogene boundary at Walvis Ridge (ODP Hole 1262C, South Atlantic
525 Ocean), *Palaeogeography, Palaeoclimatology, Palaeoecology*, 255(1), 132-156.
- 526 Bohor, B.F., Foord, E.E., Modreski, P.J., Triplehorn, D.M., 1984. Mineralogic evidence for an
527 impact event at the Cretaceous–Tertiary boundary. *Science* 224, 867–869.
- 528 Bohor, B.F., Foord, E.E., and Betterton, W.J. (1989) Trace minerals in K-T boundary clays:
529 *Meteoritics* 24, 253.
- 530 Bohor, B.F. and W.J. Betterton. 1993. Arroyo el Mimbral, Mexico, K/T unit; origin as debris flow/
531 turbidite, not a tsunami deposit. *Proceedings of the lunar and planetary science conference*,
532 24, 143-144.
- 533 Bohor, B.F., Betterton, W.J., Krogh, T.E., 1993. Impact-shocked zircons: discovery of shock-
534 induced textures reflecting increasing degrees of shock metamorphism. *Earth Planet. Sci.*
535 *Lett.* 119, 419–424.
- 536 Bohor B.F. and Glass B.P. (1995) Origin and diagenesis of K/T impact spherules – From Haiti to
537 Wyoming and beyond. *Meteoritics* 30, 182–198.
- 538 Bourgeois J., Hansen T.A., Wiberg P.L., Kauffman E.G. (1988) A tsunami deposit at the
539 cretaceous-tertiary boundary in Texas. *Science* 241. p.567–570.
- 540 Bown, P. (2005), Selective calcareous nannoplankton survivorship at the Cretaceous-Tertiary
541 boundary, *Geology*, 33(8), 653-656.
- 542 Bown, P.R., J.A. Lees, and J.R. Young (2004), Calcareous nannoplankton evolution and diversity
543 through time, in *Coccolithophores*, edited, pp. 481-508, Springer.

- 544 Bralower, T., Paull, C.K., Leckie, R.M., 1998. The Cretaceous–Tertiary boundary cocktail:
545 Chicxulub impact triggers margin collapse and extensive gravity flows. *Geology* 26, 331–
546 334.
- 547 Bralower, T.J., Silva, I.P. and Malone, M.J., 2002. New evidence for abrupt climate change in the
548 Cretaceous and Paleogene: An Ocean Drilling Program expedition to Shatsky Rise,
549 northwest Pacific. *GSA TODAY*, 12, pp.4-10.
- 550 Buffler, R.T., Schlager, W., Pisciotto, K.A., and Leg 77 Scientists (1984). *Initial Reports of the Deep Sea*
551 *Drilling Project 77* Washington.
- Christeson et. al., 2018 Extraordinary Rocks from the Peak Ring of the Chicxulub Impact Crater:
P-Wave Velocity, Density, and Porosity Measurements from IODP/ICDP Expedition 364,
EPSL, *in press*.
- Cintala, M.J., and Grieve, R.A. (1998). Scaling impact melting and crater dimensions: Implications
for the lunar cratering record. *Meteoritics & Planetary Science*, 33(4), 889-912.
- 552 Claeys, P., Kiessling, W., Alvarez, W., 2002. Distribution of Chicxulub ejecta at the Cretaceous–
553 Tertiary boundary. In: Koeberl, C., MacLeod, K.G. (Eds.), *Catastrophic Events and Mass*
554 *Extinctions; Impacts and Beyond: Geological Society of America Special Paper*, 356, pp.
555 55–68.
- 556 Cockell, C.S., Marco J.L. Coolen, Kliti Grice, Bettina Schaefer, Luzie Schnieders, Joanna V.
557 Morgan, Sean P.S. Gulick, Johanna Lofi, David A. Kring, and IODP-ICDP Expedition 364
558 Science Party, *submitted*, Shaping of the present-day deep biosphere by the impact
559 catastrophe that ended the Cretaceous
- 560 Collins, G.S., N. Patel, A.S. Rae, T.M. Davies, J.V. Morgan, S.P.S. Gulick and Expedition 364
561 Scientists (2017), Numerical Simulations of Chicxulub crater formation by oblique impact,
562 *Lunar Planet. Sci. Conf. XLVII*, abstr # 1832.
- 563 Coxall, H.K., S. D'Hondt, and J.C. Zachos (2006), Pelagic evolution and environmental recovery
564 after the Cretaceous-Paleogene mass extinction, *Geology*, 34(4), 297-300.
- 565 Croskell, M., Warner, M., Morgan, J., 2002. Annealing of shocked quartz during atmospheric
566 reentry. *Geophys. Res. Lett.* 29, 1940–1944.
- 567 D'Hondt, S., & Keller, G. (1991). Some patterns of planktic foraminiferal assemblage turnover at
568 the Cretaceous-Tertiary boundary. *Marine Micropaleontology*, 17(1-2), 77-118.
- 569 D'Hondt, S., Donaghay, P., Zachos, J.C., Luttenberg, D., and Lindinger, M. (1998). Organic carbon
570 fluxes and ecological recovery from the Cretaceous-Tertiary mass extinction. *Science*, 282,
571 276-279.
- 572 Denne, R.A., Scott, E.D., Eickhoff, D.P., Kaiser, J.S., Hill, R.J., and Spaw, J.M. (2013). Massive
573 Cretaceous-Paleogene boundary deposit, deep-water Gulf of Mexico: New evidence for
574 widespread Chicxulub-induced slope failure. *Geology*, 41(9), 983-986.
- 575 Ebel D.S. and L. Grossman, 2005 Spinel-bearing spherules condensed from the Chicxulub impact-
576 vapor plum, *Geology* 33, 293-296, DOI: 10.1130/G21136.1
- 577 Ekholm, A.G., and H.J. Melosh (2001), Crater features diagnostic of oblique impacts: The size
578 and position of the central peak, *Geophys. Res. Lett.*, 28, 623– 626.

- 579 Fraass, A.J., Kelly, D.C., & Peters, S.E. (2015). Macroevolutionary history of the planktic
580 foraminifera. *Annual Review of Earth and Planetary Sciences*, 43, 139-166.
- 581 Glass B.P., and Burns C.A., (1988), Mikrokrystites: a new term for impact-produced glassy
582 spherules containing primary crystallites, In: Proceedings of Lunar and Planetary Science
583 Conference, 18, 455-458.
- 584 Goldin T.J. and Melosh H.J. (2007). Interactions between Chicxulub ejecta and the Atmosphere:
585 The Deposition of the K/T Double Layer. In 38th Lunar and Planetary Science Conference,
586 pp. 2114, #1338.
- 587 Goldin and Melosh, 2008. Chicxulub ejecta distribution, patchy or continuous? In 39th Lunar
588 and Planetary Science Conference, #2469.
- 589 Gulick, S.P.S., G.L. Christeson, P.J. Barton, R.A.F. Grieve, J.V. Morgan, and J. Urrutia-
590 Fucugauchi (2013), Geophysical characterization of the Chicxulub impact crater, *Rev.*
591 *Geophys.*, 51, 31-52, doi: 10.1002/rog.200007.
- 592 Gulick, S.P.S. et al. (2016), *Expedition 364 Preliminary Report: Chicxulub: Drilling the K-Pg*
593 *Impact Crater*, International Ocean Discovery Program, doi:10.14379/iodp.pr364.2017
- 594 Gulick et al., The first Day of the Cenozoic, *in prep*
- 595 Grajales-Nishimura, Cedillo-Pardo, E., Rosales-Domínguez, C., Morán-Zenteno, D. J., Alvarez,
596 W., Claeys, P., Ruíz-Morales, J., García-Hernández, J., Padilla-Avila, P., and Sánchez-
597 Ríos, A., (2000), Chicxulub impact: The origin of reservoir and seal facies in the
598 southeastern Mexico oil fields, *Geology*; 28. 307–310.
- 599 Harwood, D.M. (1988), Upper Cretaceous and lower Paleocene diatom and silicoflagellate
600 biostratigraphy of Seymour Island, eastern Antarctic Peninsula, *Geological Society of*
601 *America Memoirs*, 169, 55-130.
- 602 Henehan, M.J., P.M. Hull, D.E. Penman, J.W. Rae, and D.N. Schmidt (2016), Biogeochemical
603 significance of pelagic ecosystem function: an end-Cretaceous case study, *Phil. Trans. R.*
604 *Soc. B*, 371(1694), 20150510.
- 605 Hildebrand, A.R., Penfield, G.T., Kring, D.A., Pilkington, M., Camargo, A.Z., Jacobsen, S.B.,
606 Boynton, W.V., 1991. Chicxulub Crater: a possible Cretaceous/Tertiary boundary impact
607 crater on the Yucatán Peninsula, Mexico. *Geology* 19, 867–871.
- 608 Hildebrand, A.R., et al. (1998), Mapping Chicxulub crater structure with overlapping gravity and
609 seismic surveys, *Proc. Lunar Planet Sci Conf.*[CD-ROM], 29, 1821.
- 610 Hollis, C.J. (1997), Cretaceous-Paleocene Radiolaria from eastern Marlborough, New Zealand,
611 Institute of Geological & Nuclear Sciences.
- 612 Hollis, C.J., and Strong, C.P. (2003). Biostratigraphic review of the Cretaceous/Tertiary boundary
613 transition, mid-Waipara river section, North Canterbury, New Zealand. *New Zealand*
614 *Journal of Geology and Geophysics*, 46 (2), 243-253.
- 615 Hsü, K.J., & McKenzie, J.A. (1985). A “Strangelove” ocean in the earliest Tertiary. *The Carbon*
616 *Cycle and Atmospheric CO: Natural Variations Archean to Present*, 487-492.

- 617 Huber, B.T., Hobbs, R.W., & Bogus, K.A. (2018). Expedition 369 Preliminary Report: Australia
618 Cretaceous climate and tectonics. International Ocean Discovery Program. Tectonic,
619 paleoclimate, and paleoceanographic history of high-latitude southern margins of Australia
620 during the Cretaceous. 26 September–26 November 2017.
- 621 Hull, P.M., and R.D. Norris (2011), Diverse patterns of ocean export productivity change across
622 the Cretaceous-Paleogene boundary: New insights from biogenic barium,
623 *Paleoceanography*, 26(3).
- 624 Hull, P.M., R.D. Norris, T.J. Bralower, and J.D. Schueth (2011), A role for chance in marine
625 recovery from the end-Cretaceous extinction, *Nature Geoscience*, 4(12), 856.
- 626 Jiang, M. J., & Gartner, S. (1986). Calcareous nanofossil succession across the
627 Cretaceous/Tertiary boundary in east-central Texas. *Micropaleontology*, 232-255.
- 628 Jiang, S., T.J. Bralower, M.E. Patzkowsky, L.R. Kump, and J.D. Schueth (2010), Geographic
629 controls on nanoplankton extinction across the Cretaceous/Palaeogene boundary, *Nature*
630 *Geoscience*, 3(4), 280.
- 631 Kamo, S.L., Lana. C., Morgan, J.V., (2011) U–Pb ages of shocked zircon grains link distal K–Pg
632 boundary sites in Spain and Italy with the Chicxulub impact, *Earth and Planetary Science*
633 *Letters* 310 401–408.
- 634 Kasting, James F. "Earth's early atmosphere." *Science* 259, no. 5097 (1993): 920-926.
- 635 Keller, G., Adatte, T., Stinnesbeck, W., Rebolledo-Vieyra, M., Urrutia-Fucugauchi, J., Kramar,
636 U., Stüben, D., 2004. Chicxulub impact predates the K–T boundary mass extinction. *Proc.*
637 *Natl. Acad. Sci.* 101, 3753–3758.
- 638 Keller, G., Adatte, T., Berner, Z., Harting, M., Baum, G., Prauss, M., Tantawy, A., Stueben, D.,
639 2007, Chicxulub impact predates K–T boundary, new evidence from Brazos, Texas, *EPSL*
640 255, 339-356.
- 641 Kennett, D.J., Kennett, J.P., West, A., Mercer, C., Hee, S.Q., Bement, L., Bunch, T.E., Sellers, M.
642 and Wolbach, W.S., 2009. Nanodiamonds in the Younger Dryas boundary sediment layer.
643 *Science*, 323, 94-94.
- 644 Kirchner, J.W., and Weil, A. (2000). Delayed biological recovery from extinctions throughout the
645 fossil record *Nature* 404, 177-180.
- 646 Klaus, A., R.D. Norris, D. Kroon, and J. Smit (2000), Impact-induced mass wasting at the KT
647 boundary: Blake Nose, western North Atlantic, *Geology*, 28(4), 319-322.
- 648 Koeberl C. 1998. Identification of meteoritic component in impactites. In *Meteorites: Flux with*
649 *time and impact effects*, edited by Grady M. M., Hutchinson R., McCall G. J. H., and
650 Rothery R. A. London: The Geological Society. pp. 133–153.
- 651 Kring, D.A., Impact events and their effect on the origin, evolution, and distribution of life, *GSA*
652 *Today* 10, 1–7 (2000).
- 653 Kring, D.A., Environmental consequences of impact cratering events as a function of ambient
654 conditions on Earth, *Astrobiology* 3, 133–152 (2003).

- 655 Kring DA, Claeys P, Gulick SPS, Morgan JV, Collins GS, Bralower T, Chenot E, Christeson G,
656 Cockell C, Coolen MJL, Ferrière L, Gebhardt C, Goto K, Jones H, Lofi J, Lowery C,
657 Mellett C, Ocampo-Torres R, Perez-Cruz L, Pickersgill A, Poelchau M, Rae A, Rasmussen
658 C, Rebolledo-Vieyra M, Riller U, Sato H, Smit J, Tikoo S, Tomioka N, Urrutia-Fucugauchi
659 J, Whalen M, Wittmann A, Xiao L, Yamaguchi KE, Zylberman Wclose, 2017, Chicxulub
660 and the exploration of large peak-ring impact craters through scientific drilling, *GSA*
661 *Today*, Vol: 27, Pages: 4-8, ISSN: 1052-5173
- 662 Krogh, T.E., Kamo, S.L., Bohor, B.F., 1993. U–Pb ages of single shocked zircons linking distal
663 K–T ejecta to the Chicxulub crater. *Nature* 366, 731–734.
- 664 Kump, L.R. (1991), Interpreting carbon-isotope excursions: Strangelove oceans, *Geology*, 19(4),
665 299-302.
- 666 Kyte, F.T., Smit, J., Wasson, J.T., 1985. Siderophile inter-element variation in the Cretaceous–
667 Tertiary boundary sediments from Caravaca, Spain. *Earth Planet. Sci. Lett.* 73, 183–195.
- 668 Kyte, F.T. and J. Smit. 1986. Regional variations in spinel compositions; an important key to the
669 Cretaceous/ Tertiary event. *Geology*, 14, 6, 485-487.
- 670 Kyte F.T, Bostwick J.A. 1995. Magnesioferrite spinel in Cretaceous/Tertiary boundary sediments
671 of the Pacific basin: remnants of hot, early ejecta from the Chicxulub impact? *Earth Planet.*
672 *Sci. Lett.* 132, 113–27.
- 673 Kyte, F.T. (1998), A meteorite from the Cretaceous/Tertiary boundary, *Nature*, 396(6708), 237.
- 674 Kyte, F.T., (2004). Primary mineralogical and chemical characteristics of the major K/T and Late
675 Eocene impact deposits. AGU Fall Meeting, abstract #B33C-0272.
- 676 Lowery et al., 2018, Rapid Recovery of Life At Ground Zero of the End Cretaceous Mass
677 Extinction, *Nature* v. 558, p. 288-291, <https://doi.org/10.1038/s41586-018-0163-6>
- 678 Luterbacher H.P & Premoli Silva I. (1964) - Biostratigrafia del limite Cretaceo-Terziario
679 nell'Apennino Centrale. *Riv. It. Paleont. Strat.*, 70, p. 67-128, Milano.
- 680 MacLeod, N., P. Rawson, P. Forey, F. Banner, M. Boudagher-Fadel, P. Bown, J. Burnett, P.
681 Chambers, S. Culver, and S. Evans (1997), The Cretaceous-tertiary biotic transition,
682 *Journal of the Geological Society*, 154(2), 265-292.
- 683 MacLeod, K.G., Whitney, D.L., Huber, B.T. and Koeberl, C., 2007. Impact and extinction in
684 remarkably complete Cretaceous-Tertiary boundary sections from Demerara Rise, tropical
685 western North Atlantic. *Geological Society of America Bulletin*, 119(1-2), pp.101-115.
- 686 McDonald, M.A., H.J. Melosh, and S.P.S. Gulick (2008), Oblique impacts and peak ring position:
687 Venus and Chicxulub, *Geophysical Research Letters*, vol. 35, L07203,
688 doi:10.1029/2008GL033346, 2008
- 689 Meisel, T, U. Kraehenbuehl and M.A. Nazarov. 1995. Combined osmium and strontium isotopic
690 study of the Cretaceous-Tertiary boundary at Sumbar, Turkmenistan; a test for an impact
691 versus a volcanic hypothesis. *Geology*, 23, 4, 313-316.
- 692 Melosh, H.J. *Impact and Explosion Cratering* (Pergamon Press, 1977).

693 Melosh, H.J., N.M. Schneider, K.J. Zahnle, and D. Latham (1990), Ignition of global wildfires at
694 the Cretaceous-Tertiary boundary, *Nature*, 343, 251-254.

695 Meredith, Robert W., Jan E. Janecka, John Gatesy, Oliver A. Ryder, Colleen A. Fisher, Emma C.
696 Teeling, Alisha Goodbla et al. "Impacts of the Cretaceous Terrestrial Revolution and KPg
697 extinction on mammal diversification." *Science* (2011): 1211028.

698 Michel, H.V., F. Asaro, W. Alvarez, and L.W. Alvarez (1986), 12. GEOCHEMICAL STUDIES
699 OF THE CRETACEOUS-TERTIARY BOUNDARY IN ODP HOLES 689B AND 690C1,
700 paper presented at Proceedings of the Ocean Drilling Program: Scientific Results v. 113

701 Montanari, A., R.L. Hay, J. Smit et al., (1983). "Spheroids at the Cretaceous-Tertiary boundary
702 are altered impact droplets of basaltic composition." *Geology* 11: 668-671.

703 Montanari, A., Koeberl, C., 2000. *Impact Stratigraphy: The Italian Record*. Lecture and Notes in
704 Earth Sciences. Springer-Verlag, Berlin. 364 pp.

705 Morgan, J., Warner, M., Brittan, J., Buffler, R., Camargo, A., Christeson, G. and Mackenzie, G.
706 (1997). Size and morphology of the Chicxulub impact crater. *Nature*, 390, 472-476.

707 Morgan, J., & Warner, M. (1999). Chicxulub: The third dimension of a multi-ring impact
708 basin. *Geology*, 27(5), 407-410.

709 Morgan J.V., Lana C., Kearsley A., Coles B., Belcher C., Montanari S., Di'az-Martí'nez E.,
710 Barbosa A. and Neumann V. (2006) Analyses of shocked quartz at the global K-P
711 boundary indicate an origin from a single, high-angle, oblique impact at Chicxulub. *Earth*
712 *Planet. Sci. Lett.* 251(3-4), 264-279.

713 Morgan J, Artemieva N, Goldin T, 2013, Revisiting wildfires at the K-Pg boundary, *Journal of*
714 *Geophysical Research: Biogeosciences*, Vol: 118, Pages: 1508-1520, ISSN: 2169-8953

715 Morgan J.V. and 34 others, 2016, The formation of peak rings in large impact craters, *SCIENCE*,
716 Vol: 354, Pages: 878-882, ISSN: 0036-8075

717 Morgan, J.V., S.P.S. Gulick, C.L. Mellet, S.L. Green, and Expedition 364 Scientists (2017)
718 *Chicxulub: Drilling the K-Pg Impact Crater, Proceedings of the International Ocean*
719 *Discovery Program, 364*, International Ocean Discovery Program, College Station, TX,
720 doi: 10.14379/iodp.proc.364.103.2017.

721 Murray, J.B. (1980). Oscillating peak model of basin and crater formation. *The moon and the*
722 *planets*, 22(3), 269-291.

723 Nisbet, E.G., and N.H. Sleep. "The habitat and nature of early life." *Nature* 409, no. 6823 (2001):
724 1083.

725 Norris, R. D., J. Firth, J. S. Blusztajn, and G. Ravizza (2000), Mass failure of the North Atlantic
726 margin triggered by the Cretaceous-Paleogene bolide impact, *Geology*, 28(12), 1119-1122.

727 Officer, C.B. and Drake, C.L. (1985). Terminal Cretaceous environmental events. *Science*, 227,
728 1161-1167.

- 729 Orth, C. J., J. S. Gilmore, J. D. Knight, C. L. Pillmore, R. H. Tschudy and J. E. Fassett (1981), An
730 iridium abundance anomaly at the palynological Cretaceous-Tertiary boundary in northern
731 New Mexico. *Science*, 214, 4527, 1341-1343.
- 732 Paquay, F.S., Ravizza, G.E., Dalai, T.K., & Peucker-Ehrenbrink, B. (2008). Determining
733 chondritic impactor size from the marine osmium isotope record. *Science*, 320(5873), 214-
734 218.
- 735 Penfield, G.T., and A. Camargo-Zanoguera, Definition of a major igneous zone in the central
736 Yucathn platform with aeromagnetics and gravity, in Technical Program, Abstracts and
737 Bibliographies, 51st Annual Meeting, p.37, Society of Exploration Geophysicists, Tulsa,
738 Okla.
- 739 Perch-Nielsen, K. (1977), Albian to Pleistocene calcareous nannofossils from the western South
740 Atlantic, DSDP Leg 39, Initial Reports of the Deep Sea Drilling Project, 39, 699-823.
- 741 Perch-Nielsen, K., J. McKenzie, and Q. He (1982), Biostratigraphy and isotope stratigraphy and
742 the 'catastrophic' extinction of calcareous nannoplankton at the Cretaceous/Tertiary
743 boundary, Geological implications of impacts of large asteroids and comets on the Earth,
744 190, 353-371.
- 745 Percival, S.F. and Fischer, A.G. (1972), Changes in calcareous nanno-plankton in the Cretaceous-
746 Tertiary biotic crisis at Zumay, Spain, *Evolutionary Theory* 2, 1-35.
- 747 Peucker-Ehrenbrink, B., and Ravizza, G. (2000). The marine osmium isotope record. *Terra*
748 *Nova*, 12(5), 205-219.
- 749 Peucker-Ehrenbrink, B., and Ravizza, G. (2012). Osmium isotope stratigraphy. In *The geologic*
750 *time scale* (pp. 145-166).
- 751 Poag, C.W., Powars, D.S., Poppe, L.J., & Mixon, R.B. (1994). Meteoroid mayhem in Ole
752 Virginny: Source of the North American tektite strewn field. *Geology*, 22(8), 691-694.
- 753 Poirier, A., and Hillaire-Marcel, C. (2011). Improved Os-isotope stratigraphy of the Arctic
754 Ocean. *Geophysical Research Letters*, 38(14).
- 755 Pollastro, R.M. and B. F. Bohor. 1993. Origin and clay-mineral genesis of the Cretaceous-Tertiary
756 boundary unit, Western Interior of North America. *Clays and Clay Minerals*, 41, 1, 7-25.
- 757 Pospichal, J. J., and S.W. Wise Jr (1990), 37. PALEOCENE TO MIDDLE EOCENE
758 CALCAREOUS NANNOFOSSILS OF ODP SITES 689 AND 690, MAUD RISE,
759 WEDDELL SEA1.
- 760 Premoli Silva, I., and H. Bolli „1973, Late Cretaceous to Eocene planktonic foraminifera, and
761 stratigraphy of Leg 15, Initial reports of the Deep Sea Drilling Project, 15, 499-547.
- 762 Rampino, M. R., & Stothers, R. B. 1984. Terrestrial mass extinctions, cometary impacts and the
763 Sun's motion perpendicular to the galactic plane. *Nature*, 308, 709-712.
- 764 Ravizza, G., Blusztajn, J., & Prichard, H. M. (2001). Re-Os systematics and platinum-group
765 element distribution in metalliferous sediments from the Troodos ophiolite. *Earth and*
766 *Planetary Science Letters*, 188(3-4), 369-381.

- 767 Reimold, W.U., Ferrière, L., Deutsch, A., & Koeberl, C. (2014). Impact controversies: Impact
768 recognition criteria and related issues. *Meteoritics and Planetary Science*, **49**, 723–731.
- 769 Renne, P.R., Deino, A.L., Hilgen, F.J., Kuiper, K.F., Mark, D.F., Mitchell, W.S., Morgan, L.E.,
770 Mundil, R., and Smit, J., 2013, Time scales of critical events around the Cretaceous-
771 Paleogene boundary: *Science*, v. 339, p. 684–687, <https://doi.org/10.1126/science.1230492>
- 772 Renne, P.R., Ignacio Arenillas, José A. Arz, Vivi Vajda, Vicente Gilabert, and Hermann D.
773 Bermúdez, Multi-proxy record of the Chicxulub impact at the Cretaceous-Paleogene
774 boundary from Gorgonilla Island, Colombia, *Geology*, *in press*.
- 775 Riller, U., Michael H. Poelchau, Auriol S.P. Rae, Felix M. Schulte, H. Jay Melosh, Gareth S.
776 Collins, Richard A.F. Grieve, Joanna V. Morgan, Sean P.S. Gulick, Johanna Lofi, Naoma
777 McCall, David A. Kring, and IODP-ICDP Expedition 364 Science Party Rock fluidization
778 during peak ring formation of large impact craters, in review at *Nature*
- 779 Robin, E., D. Boclet, P. Bonte, L. Froget, C. Jehanno and R. Rocchia. 1991. The stratigraphic
780 distribution of Ni-rich spinels in the Cretaceous-Tertiary boundary rocks at El Kef
781 (Tunisia), Caravaca (Spain) and 761C (Leg 122). *Earth and Planetary Science Letters*, 107,
782 3-4, 715-721.
- 783 Robinson, N., Ravizza, G., Coccioni, R., Peucker-Ehrenbrink, B. and Norris, R., 2009. A high-
784 resolution marine 187 Os/188 Os record for the late Maastrichtian: Distinguishing the
785 chemical fingerprints of Deccan volcanism and the KP impact event. *Earth and Planetary
786 Science Letters*, 281(3), pp.159-168.
- 787 Rocchia, R., D. Boclet, P. Bonte, L. Froget, B. Galbrun, C. Jehanno and E. Robin. 1992. Iridium
788 and other element distributions, mineralogy, and magnetostratigraphy near the Cretaceous/
789 Tertiary boundary in Hole 761C. *Proceedings of the Ocean Drilling Program, Scientific
790 Results*, 122, 753-762.
- 791 Rocchia, R., E. Robin, L. Froget, and J. Gayraud, 1996, Stratigraphic distribution of extraterrestrial
792 markers at the Cretaceous-Tertiary boundary in the Gulf of Mexico area: Implications for
793 the temporal complexity of the event, in G. Ryder, D. Fastovsky and S. Gartner, eds., *The
794 Cretaceous-Tertiary boundary event and other catastrophes in earth history: Geological
795 Society of America Special Paper 307*, Boulder, Colorado, p. 279–286.
- 796 Röhl, U., J. G. Ogg, T. L. Geib, and G. Wefer (2001), *Astronomical calibration of the Danian time
797 scale*, Geological Society, London, *Special Publications*, 183(1), 163-183.
- 798 Romein, A. (1977), Calcareous nannofossils from Cretaceous-Tertiary boundary interval in
799 Barranco del Gredero (Caravaca, Prov-Murcia, SE Spain). *Proceedings of the Koninklijke
800 Nederlandse Akademie van Wetenschappen Series B-Palaeontology Geology Physics
801 Chemistry Anthropology*, v. 80, p. 256.
- 802 Sanford, J.C., J.W. Snedden, and S.P. Gulick (2016), The Cretaceous-Paleogene boundary deposit
803 in the Gulf of Mexico: Large-scale oceanic basin response to the Chicxulub impact, *Journal
804 of Geophysical Research: Solid Earth*, 121(3), 1240-1261.
- 805 Schaller, M.F., Fung, M.K., Wright, J.D., Katz, M.E., and Kent, D.V. (2016), Impact ejecta at the
806 Paleocene-Eocene boundary, *Science* 354, 225-229.

- 807 Schueth, J. D., T. J. Bralower, S. Jiang, and M. E. Patzkowsky (2015), The role of regional survivor
808 incumbency in the evolutionary recovery of calcareous nannoplankton from the
809 Cretaceous/Paleogene (K/Pg) mass extinction, *Paleobiology*, 41(4), 661-679.
- 810 Schulte P, Deutsch A, Salge T, Berndt J, Kontny A, MacLeod KG, Neuser RD, Krumm S, 2009,
811 A dual-layer Chicxulub ejecta sequence with shocked carbonates from the Cretaceous–
812 Paleogene (K–Pg) boundary, Demerara Rise, western Atlantic, *Geochimica et*
813 *Cosmochimica Acta* 73, 1180-1204.
- 814 Schulte, P. and 40 others, (2010), The Chicxulub asteroid impact and mass extinction at the
815 Cretaceous-Paleogene boundary, *Science*, 327, 1214-1218.
- 816 Schultz P.H. and D’Hondt S., (1996), Cretaceous-Tertiary (Chicxulub) impact angle and its
817 consequences, *Geology* 24, 963-967.
- 818 Scotese, C.R., 2008. The PALEOMAP project PaleoAtlas for ArcGIS, Volume 2. Cretaceous
819 paleogeographic and plate reconstructions, PALEOMAP Project.
- 820 Shukolyukov, A. and G.W. Lugmair. 1998. Isotopic evidence for the Cretaceous-Tertiary impactor
821 and its type. *Science*, 282, 5390, 927-929.
- 822 Sigurdsson, H., D’Hondt, S., Arthur, M.A., Bralower, T.J., Zachos, J.C., van Fossen, M. and
823 Channel, J.E., 1991. Glass from the Cretaceous/Tertiary boundary in Haiti. *Nature*,
824 349(6309), p.482.
- 825 Sigurdsson, H., Leckie, R.M., & Acton, G.D. (1997). Caribbean volcanism, Cretaceous/Tertiary
826 impact, and ocean climate history: synthesis of Leg 165. In *Proceedings of the Ocean*
827 *Drilling Program Initial Reports Vol. 165*, pp. 377-402.
- 828 Smit, J. and J. Hertogen (1980). An extraterrestrial event at the Cretaceous-Tertiary boundary,
829 *Nature* 285: 198-200.
- 830 Smit, J. (1982), Extinction and evolution of planktonic foraminifera at the Cretaceous/Tertiary
831 boundary after a major impact, Geological implications of impacts of large asteroids and
832 comets on the Earth: Geological Society of America Special Paper, 190, 329-352.
- 833 Smit, J. and F.T. Kyte. 1984. Siderophile-rich magnetic spheroids from the Cretaceous-Tertiary
834 boundary in Umbria, Italy. *Nature*, 310, 5976, 403-405.
- 835 Smit, J., Romein, A.J.T. 1985. A sequence of events across the Cretaceous-Tertiary boundary.
836 *Earth Planet. Sci. Lett.* 74:155–70
- 837 Smit J., Alvarez W., Montanari A., Swinburn N.H.M., Van Kempen T.M., Klaver G.T. and
838 Lustenhouwer W. J. (1992)“Tektites” and microkrystites at the Cretaceous–Tertiary
839 boundary: two strewn fields, one crater? *Lunar Planet. Sci.* 22, 87–100.
- 840 Smit, J. (1999), The global stratigraphy of the Cretaceous-Tertiary boundary impact ejecta, *Annual*
841 *Review of Earth and Planetary Sciences*, 27, 75-113.
- 842 Swisher, C.C., Grajales-Nishimura, J. M., Montanari, A., Margolis, S. V., Claeys, P., Alvarez, W.,
843 Renne, P., Cedillo-Pardo, E., Maurrasse, F. J-M. R., Curtis, G.H., Smit, J., and McWilliam,
844 M.O. (1992). Coeval ⁴⁰Ar/³⁹Ar ages of 65.0 million years ago from Chicxulub crater melt
845 rock and Cretaceous-Tertiary boundary tektites. *Science*, 257(5072), 954-958.

- 846 Thierstein, H.R. (1982), Terminal Cretaceous plankton extinctions: A critical assessment, in
847 Geological implications of impacts of large asteroids and comets on the earth, edited, pp.
848 385-399.
- 849 Thierstein, H.R., and H. Okada (1979), The Cretaceous/Tertiary boundary event in the North
850 Atlantic, Initial Reports of the Deep Sea Drilling Project, 43, 601-616.
- 851 Thomas, E., & Monechi, S. (2007). Cenozoic mass extinctions in the deep sea: What perturbs the
852 largest habitat on Earth? *Geological Society of America Special Paper*, 424, 1-23.
- 853 Turgeon, S. C., & Creaser, R. A. (2008). Cretaceous oceanic anoxic event 2 triggered by a massive
854 magmatic episode. *Nature*, 454, 323.
- 855 Westerhold, T., U. Röhl, I. Raffi, E. Fornaciari, S. Monechi, V. Reale, J. Bowles, and H. F. Evans
856 (2008), Astronomical calibration of the Paleocene time, *Palaeogeography, Palaeoclimatology, Palaeoecology*, 257(4), 377-403.
- 858 Whalen, M.T., Gulick, S.P.S., Pearson, Z. F., Norris, R.D., Perez-Cruz, L., & Urrutia-Fucugauchi,
859 J. (2013). Annealing the Chicxulub impact: Paleogene Yucatán carbonate slope
860 development in the Chicxulub impact basin, Mexico. *Deposits, Architecture, and Controls*
861 *of Carbonate Margin, Slope and Basinal Settings*. SEPM Special Publication 105, p. 282-
862 304.
- 863 Vellekoop, J., Sluijs, A., Smit, J., Schouten, S., Weijers, J.W.H., Sinninghe Damsté, J.S.,
864 Brinkhuis, H., 2014. Rapid short-term cooling following the Chicxulub impact at the
865 Cretaceous–Paleogene boundary. *PNAS* 2014, 111, 7537-7541.
- 866 Zachos, J.C., Arthur, M.A., & Dean, W.E. (1989). Geochemical evidence for suppression of
867 pelagic marine productivity at the Cretaceous/Tertiary boundary. *Nature*, 337, 61-64.